Macromolecular Materials and Engineering
Open Access
www.mame-journal.de

The Critical Role of Processing Sequence on the Mechanical Properties of Reactively Compatibilized PLA/PBAT Blends: Effect of Manufacturing Method

*Sanaz Soleymani Eil Bakhtiari, Reza Salehiyan, Anu Sasi, Islam Shyha, and Dongyang Sun**

In this study, polylactic acid (PLA)/polybutylene adipate-co-terephthalate (PBAT)/Joncryl blends are prepared via film extrusion, compression molding, and injection molding to investigate the effects of processing sequence and compatibilization on interfacial interactions and final properties. Joncryl is added at 0.5 and 1 wt.% to assess its impact on phase adhesion, crystallinity, and mechanical performance. Results reveal that the two-step blending process, where Joncryl is first reacted with either PLA or PBAT, results in more uniform dispersion and enhanced interfacial interactions compared to the single-step method. Notably, the (70/30) PLA/PBAT blend incorporating 1 wt.% Joncryl via two-step blending shows tensile strength improvements of ≈6% and 15%, and elongation increases of ≈491% and 335.5% for (PLA+1J)/PBAT and (PBAT+1J)/PLA, respectively. For injection-molded samples, 0.5 wt.% Joncryl added through two-step blending improves elongation and impact strength by ≈75% and 140% in (PBAT+0.5J)/PLA. Film-extruded samples exhibit higher tensile strength than compression-molded ones due to better phase dispersion, orientation, and interfacial bonding enabled by slit-die extrusion and stretching. In contrast, compression molding lacks orientation effects, resulting in lower mechanical strength. These findings highlight the critical role of blending sequence and processing method in tailoring biodegradable PLA/PBAT blends for improved performance in packaging and related applications.

1. Introduction

Environmental pollution poses a serious challenge to sustainable development, with packaging waste in landfills contributing significantly to environmental harm. The development of biodegradable polymers from renewable sources is seen as an effective solution to plastic waste, and their adoption as a substitute for petroleum-based plastics is increasingly recognized worldwide.[1–4] The problem of white pollution caused by conventional non-biodegradable plastics has attracted global concern for decades.[5–7] In response, many countries are now actively encouraging the use of eco-friendly polymers. The adoption of biodegradable polymers is widely regarded as an effective solution to this issue.[8–11] Polylactic acid (PLA) and polybutylene adipate-co-terephthalate (PBAT) are two of the most widely studied biodegradable polymers due to their complementary properties. PLA, a bio-based polyester, is characterized by its high stiffness, strength, and biodegradability, but suffers from inherent brittleness and poor flexibility.[3,12–15] In contrast, PBAT, a synthetic aliphatic-aromatic copolyester, exhibits excellent ductility and flexibility but lacks sufficient mechanical strength for high-performance applications. To overcome these individual limitations, blending PLA and PBAT has been explored as an effective approach to developing balanced biodegradable materials with improved mechanical properties, biodegradability, and processability.[9,16–20] Despite the potential of PLA/PBAT blends, the inherent immiscibility between PLA and PBAT due to their different polarities and molecular structures results in poor interfacial adhesion, leading to phase-separated morphologies with compromised mechanical properties.[9,21,22] Therefore, compatibilization strategies have been widely investigated to enhance the interfacial interaction between these polymers, ensuring improved mechanical performance and structural stability.[23] Compatibilization affects polymer blends through two key mechanisms: i) preventing droplet coalescence and ii) lowering interfacial tension, both leading to reduced droplet sizes. These effects are most pronounced when the compatibilizer is located at the interface.[24,25] In the absence of compatibilizers, polymer blend properties are notably inferior to those of the individual polymers. Common compatibilization strategies include i) non-reactive approaches using

S. Soleymani Eil Bakhtiari, R. Salehiyan, A. Sasi, I. Shyha, D. Sun
School of Computing
Engineering and the Built Environment
Edinburgh Napier University
Edinburgh EH10 5DT, UK
E-mail: d.sun@napier.ac.uk

The ORCID identification number(s) for the author(s) of this article can be found under https://doi.org/10.1002/mame.202500108

DOI: 10.1002/mame.202500108

co-solvents or copolymers, ii) reactive methods that create copolymers in situ, and iii) nanofiller-assisted techniques incorporating small amounts of nanofillers. The selection of a method depends on factors such as cost, performance, recyclability, and biodegradability.[26–28] One common route involves the use of reactive compatibilizers, such as multifunctional chain extenders, which promote in situ reactions between PLA and PBAT to improve interfacial adhesion.[16,29–31] Among these, epoxide-based chain extenders like Joncryl have been extensively studied for their ability to react with carboxyl (—COOH) and hydroxyl (—OH) groups, extending polymer chains and reducing phase separation.[16,29,32] Research has demonstrated that incorporating various types of Joncryl ADR, such as 4468, 4368, and 4370, into PLA/PBAT blends enhances tensile strength, elongation at break, and impact resistance. These improvements are attributed to better interfacial adhesion and an increase in molecular weight due to chain extension. For example, Wang et al.[33] developed high-strength, high-toughness PLA/PBAT (60/40) blends using a melt-reactive blending approach. By introducing Joncryl ADR-4370S as a compatibilizer through an in situ compatibilization reaction, its epoxy groups and the terminal carboxyl and hydroxyl groups of PLA and PBAT, forming a PLA-g-PBAT copolymer linking the two segments. This reaction notably reduced the interfacial tension between the phases. They achieved enhanced mechanical properties across all blends.[33] In another study, Al-Itry et al.[34] evaluated the effect of multifunctional epoxide (Joncryl;ADR-4368) on the interfacial properties of biopolymer blends based on PLA/PBAT. The results indicated a decrease in interfacial tension in the modified/compatibilized PLA/PBAT blend and the formation of the PLA-Joncryl-PBAT copolymer, leading to enhanced mechanical properties.[34] Arruda et al.[16] studied the influence of Joncryl ADR 4368 on PLA/PBAT blend and found that for the 60 PLA blend, the addition of a chain extender resulted in a 900% increase in elongation at break compared to the 60PLA blend without it. Additionally, it exhibited a 1200% increase relative to neat PLA, significantly enhancing ductility. Moreover, in the 60 PLA blends containing a chain extender, the dispersed phase was refined, transitioning from coarse sheets or platelets to elongated PBAT fibrils. This morphological transformation is likely responsible for the increased elongation at break. Additionally, a notable enhancement in stress at break was observed, rising from 22.3 MPa (without a chain extender) to 34–35 MPa with its addition.[16] However, the effectiveness of Joncryl in modifying PLA/PBAT blends is highly dependent on processing conditions. Previous research has primarily focused on single-step blending methods, where all components are processed simultaneously. While this method can enhance interfacial adhesion to some extent, limitations such as incomplete reactions and phase inhomogeneity still persist.

Recent efforts have explored two-step blending strategies as an alternative approach to improve the dispersion and reaction efficiency of compatibilizers in PLA/PBAT blends. The two-step blending method involves pre-reacting Joncryl with either PLA or PBAT before incorporating the second polymer, allowing for better dispersion of Joncryl, molecular interaction, and controlled compatibilization. This method is expected to lead to a more uniform morphology, enhanced chain extension, and improved mechanical performance. In this work, we investigate the impact of blending sequence on the compatibilization efficiency of Joncryl-modified PLA/PBAT blends by comparing single-step and two-step blending approaches. Due to the different reactivity of Joncryl toward PLA and PBAT, with a higher reactivity toward PLA because of its greater number of terminal groups,[16] we aim to investigate the effect of blending sequence. Specifically, we evaluate the impact of pre-reacting Joncryl with PLA and PBAT to understand how this pre-compatibilization influences the final blend morphology and properties. Through Fourier Transform Infrared Spectroscopy (FTIR), mechanical testing, and morphological analysis, we aim to provide a comprehensive understanding of how processing sequences affect the interfacial interactions and final performance of the blends. By correlating spectroscopic findings with mechanical properties such as tensile strength, elongation at break, and impact resistance, we assess the effectiveness of Joncryl as a reactive compatibilizer under different processing conditions.

A key novelty of this study is the detailed comparison between injection molding and film/sheets extrusion processes in influencing the chemical interactions between Joncryl and PLA/PBAT components. Injection molding typically involves shorter residence times (≈60 s), potentially leading to incomplete reactions and higher residual unreacted Joncryl. On the other hand, melt extrusion involves longer thermal exposure (≈180–190 °C) for extended durations, facilitating more complete reactions and uniform dispersion of the compatibilizer. By examining these different processing methods, this study provides crucial insights into optimizing compatibilization strategies for PLA/PBAT blends.

Table 1. Thermal properties of the PLA and PBAT.

Polymer	Grade	MFI [190 °C/2.16 kg]	Tg [°C]	Tm [°C]
PLA	Luminy L130	10 g/10 min	60	175
PBAT	≥ 99% (L-isomer) ecoflex F Blend C1200	2.7–4.9 g/10 min	−30	110–120

2. Experimental Section

2.1. Materials

PLA pellets (Luminy L130) was supplied from TotalEnergies Corbion (The Netherlands). PBAT ecoflex F Blend C1200 was kindly supplied by BASF Corporation (Germany). The commercial grade is characterized by a density of 1.25–1.27 g cm^{-3} and a melt flow index 2.7–4.9 g/10 min at 190 °C. Chain extender was used as a functional additive Joncryl ADR 4468, supplied by BASF (Germany). ExxonMobil low-density polyethylene (LDPE) LD 150 BW was supplied from ExxonMobil Chemicals. **Table 1** summarized the thermal properties of the polymers used in this study.[35,36]

2.2. Polymer Processing

2.2.1. Film/Sheet Extrusion

For the fabrication of films and sheets via extrusion, two processing approaches were utilized: the single-step approach and the blending sequence.

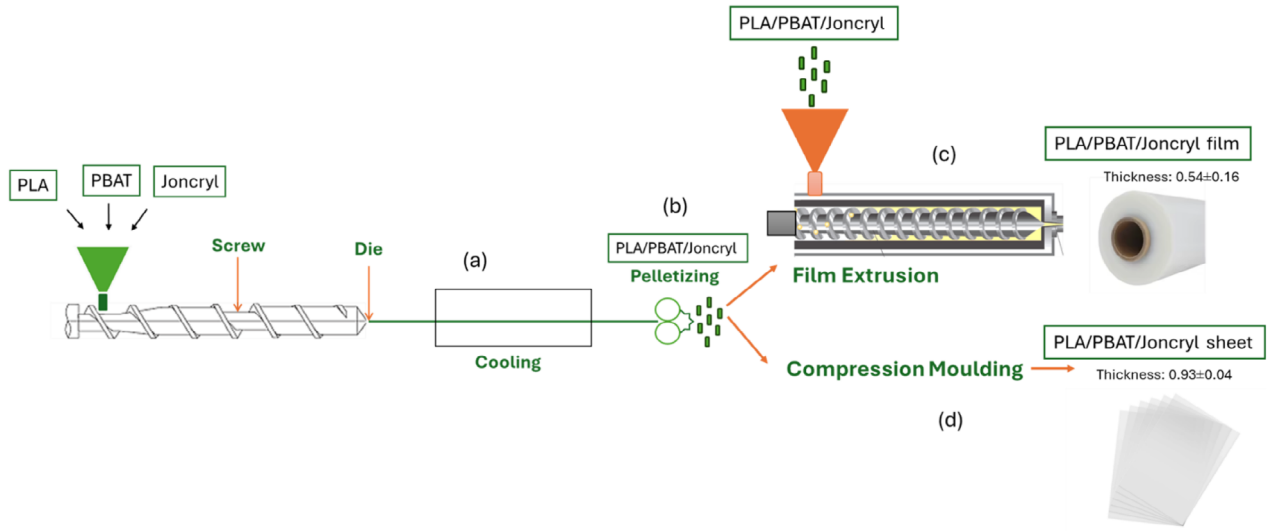

Figure 1. Single-step processing approach.

For both processing approaches, PLA and PBAT pellets were vacuum-dried at 60 °C for ≈12 h prior to use. PLA/PBAT/ Joncryl ADR 4468 blend samples, with weight ratios of 70/30, and 50/50 (wt.%/wt.%), were prepared through reactive melt blending using single screw extruder. The Joncryl ADR 4468 content was maintained at 0.5% and 1% by weight relative to the total PLA/PBAT. The profile temperature was set at 140, 150, 160, 170, 175, 180, 190 °C with a screw speed of 14 rpm. A minimum of five tensile test specimens were produced for each formulation. LDPE was used as a control material to provide a performance benchmark. LDPE was extruded using a Brabender extruder at profile temperatures of 160, 175, 185, and 190 °C as a benchmark sample, with a screw speed of 40 rpm, and a processing time of 5 min.

2.2.2. Single-Step Processing Approach

Initially, PLA, PBAT, and Joncryl ADR 4468 were fed into a single-screw extruder to produce PLA/PBAT/Joncryl filaments (**Figure** 1a).

The extruded filaments were subsequently converted into pellets using a pelletizer (Figure 1b).

The pelletized PLA/PBAT/Joncryl blends were processed into films using film extrusion, with a temperature profile of 180, 185, 190, and 190 °C, a screw speed of 40 rpm, and a processing time of 5 min (Figure 1c).

The pelletized PLA/PBAT/Joncryl blends were transformed into sheets using a hot and cold compression molding machine. The process involved hot compression at 190 °C and 20 bar pressure for 7 min, followed by cold compression at 15 bar pressure for 5 min (Figure 1d).

2.2.3. Blending Sequence Processing Approach

Initially, PLA and Joncryl or PBAT and Joncryl were fed into the single-screw extruder to produce PLA/ Joncryl or PBAT/Joncryl filaments (**Figure** 2a).

The extruded filaments were subsequently converted into pellets using a pelletizer (Figure 2b).

For producing (PLA + Joncryl)/PBAT films, PLA/Joncryl pellets and pure PBAT pellets were introduced into the film extruder. Similarly, for (PBAT + Joncryl)/PLA films, PBAT/Joncryl pellets and pure PLA pellets were fed into the film extruder (Figure 2c) with a temperature profile of 180, 185, 190, and 190 °C, a screw speed of 40 rpm, and a processing time of 5 min.

To produce (PLA + Joncryl)/PBAT compressed sheets, PLA/Joncryl pellets and pure PBAT pellets were first fed into a single-screw extruder to form filaments (Figure 2d), which were then converted into pellets using a pelletizer (Figure 2e). The resulting (PLA + Joncryl)/PBAT pellets were subsequently processed into sheets through hot and cold compression molding (Figure 2f). The process involved hot compression at 190 °C and 20 bar pressure for 7 min, followed by cold compression at 15 bar pressure for 5 min. A similar process was followed to produce (PBAT + Joncryl)/PLA compressed sheets.

2.2.4. Injection Molding

Prior to injection molding, the polymer was dried for 4 h at 60 °C in an oven to remove any absorbed moisture. Polymer pellets were processed with the help of injection molding using a Billion 50T injection molding machine at a mold temperature 60 °C. The temperature profile was set to 145 to 185 °C from the feeder to the nozzle, respectively. Joncryl was added to the blend in 0.5 and 1 wt.%. A two-step method was also employed to enhance the distribution of Joncryl within the blend. Joncryl was pre-mixed with PBAT to make PBAT/Joncryl before it was blended with PLA in an injection molding process to afford the (70/30) PLA/PBAT blends. The concentration of Joncryl was fixed at 0.5 wt.% in the two-step method to compare with the blend prepared simultaneously. A minimum of five tensile and impact test specimens were produced for each formulation. **Table** 2 presents the various routes and materials utilized for preparing injection-molded samples.

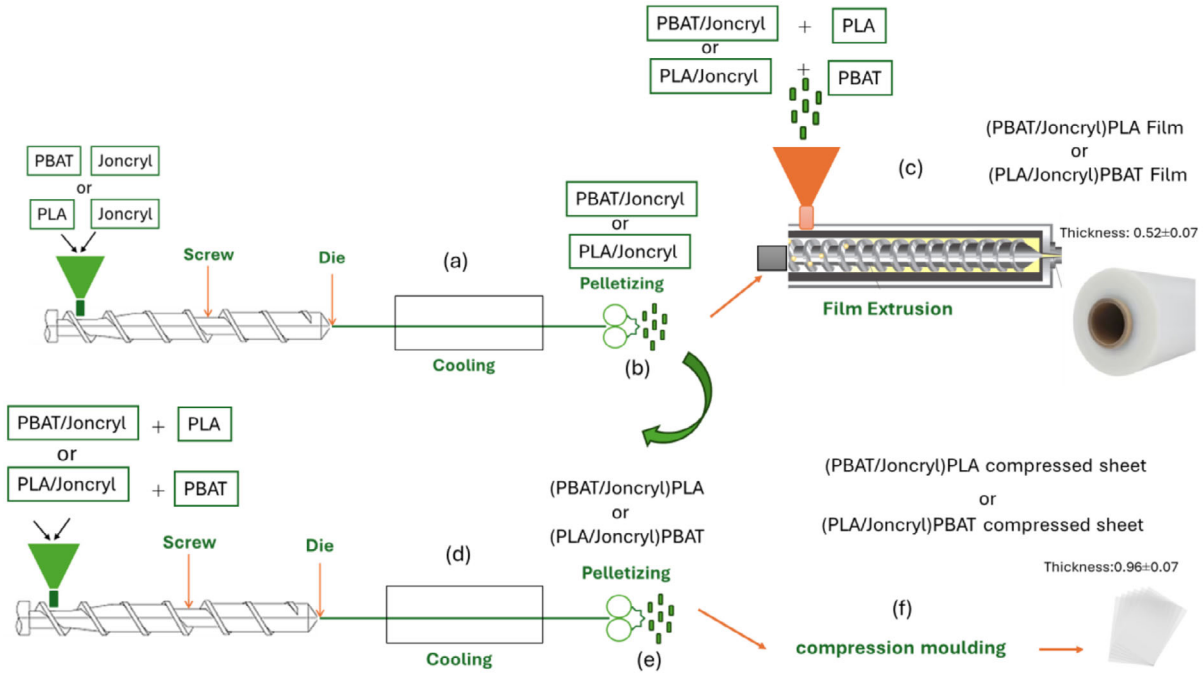

Figure 2. Blending sequence processing approach.

2.3. Physical Characterization

2.3.1. Fourier Transform Infrared (FTIR)

The FTIR (PerkinElmer Frontier, USA) was adjusted in attenuated total reflectance (ATR) mode to analyze the structural properties and characteristic peaks of PLA, PBAT, Joncryl as well as blends with and without Joncryl. Samples were scanned at a resolution of 5 cm^{-1} over a range of 400–4000 cm^{-1}.

2.3.2. Differential Scanning Calorimetry (DSC)

In order to analyze the thermal properties of modified and unmodified blends, DSC tests were carried out using a DSC Q200 (TA Instrument) under a nitrogen atmosphere. Specimens weighing between 5 and 10 mg were prepared and subjected to a heating and cooling process from −5 to 200 °C at a heating/cooling rate of 10 °C min^{-1}. The DSC analysis allowed the determination of several thermal properties, melting temperature (T_m), crystallization temperature (Tc), cold crystallization temperature (Tcc), and the heats of melting (ΔH_m). Additionally, the degree of crystallinity of PLA, denoted as $\%X_c$, was calculated using the following equation:

$$X_c\,(\%\text{crystallinity}) = \frac{\Delta H_m}{\Delta H_m^0\, \emptyset_{PLA}} \times 100 \quad (1)$$

where ΔH_m^0 is the heat of fusion of 100% crystalline PLA, which is reported as 93 J g^{-1} and ϕ_{PLA} is the weight fraction of PLA in blends.[37,38]

Table 2. Various routes and materials are utilized for preparing injection-molded samples.

Route	Materials
Single shot	PLA
Single shot	PLA/PBAT (70/30)
Single shot	PLA/PBAT/J (70/30/0.5)
Single shot	PLA/PBAT/J (70/30/1)
Two-Step	(PBAT+J)/PLA (30+0.5)/70

2.3.3. Scanning Electron Microscopy (SEM)

The fractured cross-sections of the films were examined to investigate their surface morphologies using a TESCAN VEGA SEM operated at an accelerating voltage of 10 and 20 kV. Film samples with a thickness of 0.5–1 mm were cryo-fractured by immersing them in liquid nitrogen for 1 min followed by rapid breaking. Prior to SEM imaging, the fractured cross-sections were sputter-coated with a thin layer of gold to improve surface conductivity and image quality.

2.4. Mechanical Characterization

For tensile tests, dumbbell-shaped specimens were cut from the compression-molded sheets, extruded films, and injection-molded using a press cutter and tested using Zwick tensile testers (50 and 5 kN) with computer control, following ASTM D638 for injection-molded and extruded/pressed samples, respectively. The crosshead speed was set to 5 mm min^{-1}. The dimensions of the tensile test of extruded/pressed samples were 4 mm in width and 25 mm in length, with the thickness varying for film and

compressed samples as indicated in Figures 1 and 2. Additionally, the injection-molded samples used for tensile testing measured 10 mm in width and 80 mm in length.

The Charpy impact strength of injection molded samples is determined using a B5113 Charpy impact tester (Zwick/Roell, Germany) using a 50J hammer. The specimens were produced to adhere to ISO179. The 3.7 mm thick square sheets were cut using a bandsaw to produce 80 × 10 mm specimens. Sizes were confirmed with an analogue gauge. Five specimens were prepared for each test, and a 2 mm, 45° notch was cut into the sample at the midpoint using a motorized notching machine (Ray-Ran).

3. Results and Discussion

3.1. Fourier Transform Infrared (FTIR)

The FTIR spectra of PLA and PBAT, along with their Joncryl-modified versions, reveal significant insights into the chemical interactions and structural modifications induced by the reactive chain extender. In both injection-molded and film-extruded samples, characteristic peaks associated with the functional groups in PLA and PBAT provide a basis for understanding the effect of Joncryl addition. The primary peaks of interest include the carbonyl (C═O) stretching region (1700–1750 cm^{-1}), the methylene (—CH_2) stretching region (2850–2950 cm^{-1}), and the ester-related C—O stretching region (1100–1300 cm^{-1}).[39]

In pure PLA, distinct peaks at ≈954 and 1264 cm^{-1} are observed, corresponding to C═C bending and C—O stretching vibrations in the ester groups, respectively (**Figure 3a**).[40] In PBAT, the strong carbonyl peak C═C at ≈1711 cm^{-1} and C—O at 1267 cm^{-1} represent the ester groups, while the methylene (—CH_2) rocking vibration is shown ≈729 cm^{-1} (Figure 3a').[41–44] Upon the addition of Joncryl, these peaks undergo significant modifications depending on the polymer system and processing method. In injection-molded PLA/Joncryl samples, the peaks at 954 and 1264 cm^{-1} disappear, indicating that Joncryl has altered the polymer's structural organization (See the arrow in Figure 3a). This chemical interaction likely reduces the number of free ester groups available for stretching vibrations. Similarly, the C—H stretching region (2900–3000 cm^{-1}) exhibits broadening and intensity reduction, supporting the notion that steric hindrance and molecular reorganization occur due to Joncryl's interaction with PLA.[45]

In PBAT/Joncryl injection-molded samples (Figure 3a) however, no significant spectral shifts are observed, particularly in the carbonyl (≈1711 cm^{-1}) and C—O stretching (1100–1300 cm^{-1}) regions. The peaks associated with the benzene rings [29,39] (720–900 cm^{-1}) remain unchanged, suggesting that Joncryl does not significantly alter PBAT's chemical structure in these conditions. This lack of modification in PBAT is likely due to the short thermal exposure during injection molding (≈60 s), which may limit the extent of reaction between Joncryl and PBAT's functional groups.

Conversely, in melt-extruded PBAT/Joncryl sheets, substantial spectral changes are evident (Figure 3a'). The peak at 729 cm^{-1}, linked to methylene rocking vibrations, disappears, indicating a reduction in crystalline order due to chain extension and branching.[46] The carbonyl peak at 1711 cm^{-1} weakens and slightly shifts, confirming the interaction of Joncryl's epoxy groups with PBAT's carboxyl and hydroxyl terminals. Additionally, the disappearance of peaks at 1017–1018 cm^{-1} and 1247–1270 cm^{-1} suggests significant chemical modification, likely involving the formation of new ester or ether linkages. Moreover, the intensity of peaks at ≈3000 cm^{-1} (2851–2921 cm^{-1}) representing C—H stretching in aliphatic and aromatic portions was decreased after melting extrusion (Figure 3b'). The increased thermal exposure in melt extrusion (≈180–190 °C for an extended duration) facilitates a more complete reaction of Joncryl with PBAT, reducing the presence of unreacted chain extender and leading to enhanced molecular weight and branching.

For PLA/PBAT blends, the impact of Joncryl and the processing method is particularly pronounced. In injection-molded PLA/PBAT/Joncryl samples (Figure 3c), the carbonyl peak (1700–1750 cm^{-1}) exhibits only minor changes, with a slight intensity reduction at 0.5 wt.% Joncryl and broadening at 1 wt.%. This suggests partial compatibilization, but the short processing time may limit the full extent of the reaction. In contrast, melt-extruded PLA/PBAT/Joncryl blends demonstrate more substantial spectral modifications (Figure 3c'). The carbonyl peak at 1711 cm^{-1} significantly weakens, and the peak at 1750 cm^{-1} intensifies, particularly in two-step blended samples where Joncryl is pre-reacted with PBAT before mixing with PLA (Figure 3c'). This indicates improved compatibilization and reduced phase separation. The methylene C—H peaks at 2926 and 2946 cm^{-1}, which are present in injection-molded samples, fade in the two-step melt-extruded blends, further supporting the hypothesis that extended thermal processing allows for more effective reaction and molecular integration.

The disappearance of the 2850 cm^{-1} peak and reduction of 2926–2946 cm^{-1} peaks in two-step blends provide further evidence of structural reorganization and improved phase compatibility (Figure 3d'). This enhanced interaction aligns with mechanical findings, where two-step melt-extruded PLA/PBAT/Joncryl blends exhibit higher elongation at break and superior strain-hardening behavior than the simultaneously blended ones (will be shown later). The more pronounced changes in the FTIR spectra of melt-extruded samples confirm that the longer residence time at elevated temperatures allows for greater reaction efficiency, reducing residual unreacted Joncryl compared to injection-molded samples.

The peaks observed ≈2990 cm^{-1} attributed to CH_2 stretching and the deformation of terminal C—H groups, respectively,[47] provided additional evidence of chemical interactions facilitated by Joncryl. The FTIR analysis highlights the critical role of processing conditions in determining the extent of Joncryl-induced chemical modifications in PLA, PBAT, and their blends. Injection molding, with its short exposure time, results in limited reactions, particularly in PBAT, whereas extrusion facilitates more extensive interactions, leading to increased molecular weight, branching, and improved compatibility in PLA/PBAT blends. These findings emphasize the necessity of optimizing processing conditions to maximize the effectiveness of reactive compatibilization strategies in biodegradable polymer systems.

The supplementary information on the FTIR results of blend films (50/50) and (70/30), where Joncryl was incorporated either simultaneously or sequentially via extrusion and compression molding, is provided in the supplementary document as Figures S1, S2 (Supporting Information), respectively.

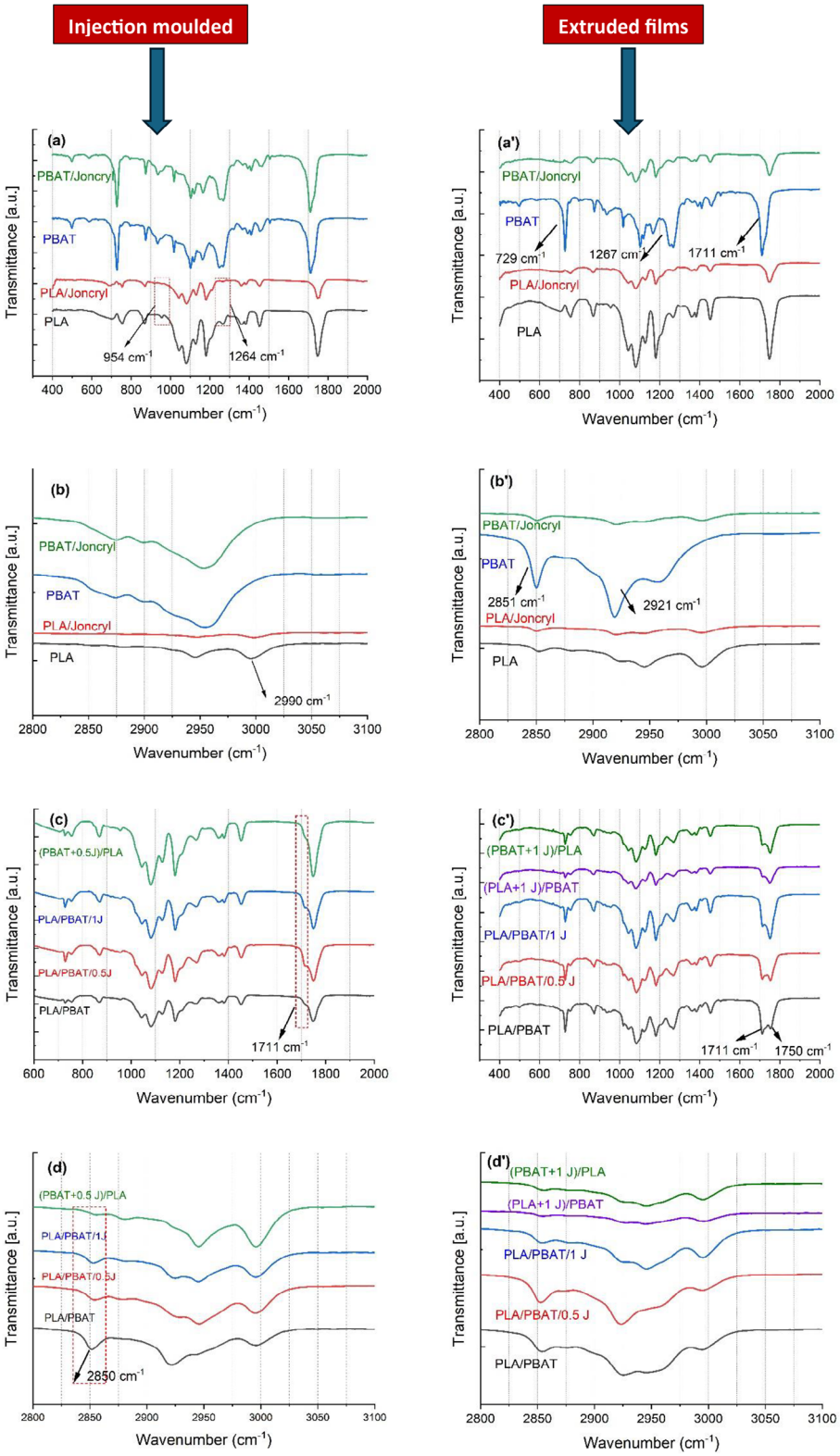

Figure 3. FTIR spectra of PLA, PBAT, PLA/J, PBAT/J, and (70/30) PLA/PBAT blends incorporating Joncryl, added either simultaneously or sequentially. Polymers and the blends were prepared via injection molding (a–d) and film extrusion (a'–d').

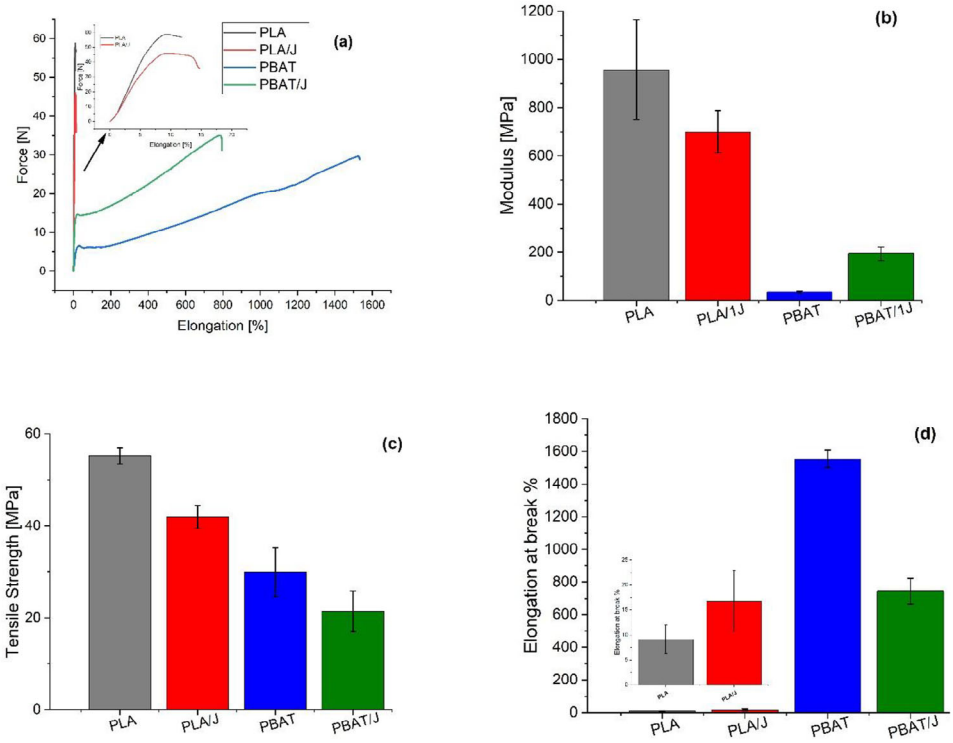

Figure 4. a) tensile curves, b) tensile modulus, c) tensile strength, and d) elongation at breaks of extruded PLA, PLA/J, PBAT, and PBAT/J films (Joncryl content was 1 wt.%).

3.2. Mechanical and Morphological Properties

The mechanical performance of PLA and PBAT films, as modified by Joncryl, provides valuable insights into the effects of reactive compatibilization on polymer chain interactions, stiffness, and elongation behavior (**Figure 4**). The modulus of PLA significantly decreases when Joncryl is introduced, as seen in Figure 4b, where the modulus drops from above 1000 MPa in neat PLA to ≈700 MPa in PLA/Joncryl. This reduction in modulus suggests that Joncryl has successfully introduced chain extension and branching, increased molecular weight, and reduced chain mobility, which ultimately makes the polymer less brittle. The FTIR results confirmed the reaction between Joncryl and PLA's terminal hydroxyl and carboxyl groups, leading to structural modifications that promote a more flexible polymer network.

The increase in elongation at break in PLA after the addition of Joncryl, as shown in Figure 4a,d, further supports this molecular-level modification. The increased elongation at break, rising from below 10% in neat PLA to nearly 20% in PLA/Joncryl, indicates that Joncryl facilitates higher energy absorption before failure, enhancing ductility. These findings confirm that reactive compatibilization through Joncryl transforms PLA from a stiff, brittle material into a more flexible and stretchable polymer, making it more suitable for applications requiring enhanced flexibility and toughness.[16] In contrast to PLA, PBAT experiences an increase in modulus after Joncryl addition, as seen in Figure 4b, where the modulus rises from below 50 MPa in PBAT to nearly 194 MPa in PBAT/Joncryl. This increase suggests that Joncryl restricts PBAT's natural flexibility, likely through minimal chain extension and branching reactions, and mostly due to the physical and hydrodynamic effects of the rigid Joncryl particles. The FTIR results for PBAT/Joncryl showed subtle but significant changes in C═O and C—O—C stretching vibrations, indicating that while PBAT is less reactive toward Joncryl compared to PLA, some level of chain extension and interfacial interaction still occurs.

The reduction in elongation at break in PBAT upon Joncryl addition, as seen in Figure 4d, confirms that Joncryl limits PBAT's ability to stretch, making it less flexible than neat PBAT. While PBAT typically exhibits high elongation at break exceeding 1500%, the addition of Joncryl reduces this value significantly. This suggests that Joncryl enhances interchain interactions and entanglements, limiting chain slippage under tensile deformation and causing earlier failure. The increase in modulus, coupled with the decrease in elongation, suggests a shift in PBAT's mechanical behavior from an ultra-flexible material to a more structured and slightly stiffer polymer, possibly due to the unreacted or partially reacted hydrodynamic effect of Joncryl particles. Given the contrasting effects of Joncryl on PLA and PBAT, it was necessary to develop a blended system that exploits the advantages of both polymers while mitigating their individual limitations. The results demonstrate that Joncryl softens PLA while stiffening PBAT, making it possible to strategically tailor the blend ratio and processing sequence to achieve an optimal balance of strength, toughness, and flexibility. By blending PLA with PBAT in the presence of Joncryl, we aimed to enhance elongation at break beyond that of neat PLA, while also improving mechanical strength beyond that of PBAT alone. The FTIR results of PLA/PBAT blends compatibilized with Joncryl confirmed that

strong interfacial interactions were achieved, further supporting the observed mechanical improvements. The choice of sequential blending methods (PBAT+J/PLA vs PLA+J/PBAT) further influenced the performance.

The tensile properties of PLA/PBAT blends prepared via film extrusion and compression molding reveal critical differences influenced by processing conditions and blend sequence (**Figure 5**). The film-extruded samples consistently exhibit higher tensile strength compared to their compression-molded counterparts, which can be attributed to the enhanced phase dispersion, orientation effects, and improved interfacial interactions facilitated by the very narrow slit die extrusion and the subsequent stretching. In contrast, compression molding of the extruded blends lacks such orientation and corresponding strain-induced strengthening, leading to lower tensile strength. During extrusion, the polymer experiences shear and elongational flow, leading to the alignment of polymer chains and improved dispersion of the minor phase, such as PBAT in PLA/PBAT blends (**Figure 6**).

Such elongational traces can be seen from the SEM images of the cryo-fractured cross-section of the sheets. This enhances tensile strength and elongation, particularly in the machine direction. Additionally, the rapid cooling in extrusion results in finer, more uniform crystallization, which contributes to improved stiffness and ductility. In contrast, compression molding involves longer static heating and pressing (12 min), leading to a more random molecular arrangement and potential phase separation, reducing mechanical performance. Extruded films are also denser and less prone to defects such as voids, which are common in compression-molded samples due to trapped air.

The blend ratio plays a significant role in determining mechanical properties, with (70/30) PLA/PBAT blend demonstrating superior tensile strength (30.9 ± 1.17 MPa) compared to its (50/50) counterparts (23.72 ± 2.1 MPa). This trend aligns with the inherent stiffness of PLA, which dominates the mechanical response as its proportion increases.[12] The (50/50) blends, being more PBAT-rich, exhibit lower tensile strength but greater flexibility, indicating that the mechanical balance of these blends is largely dictated by the polymer composition. Similar trends have been reported in other works where increasing PBAT content had negatively affected tensile strength.[33,48,49] The addition of Joncryl to these blends leads to a noticeable improvement in tensile strength, as evidenced in both processing methods.[33] Morphological changes upon Joncryl addition can be seen in **Figures 7** and **8**. It is seen in (70/30) series, blends show drastic changes from large, elongated inclusions (**Figure 8a**) into smaller inclusions in (Figure 8b,c) indicating some level of compatibilization. At 1 wt.% Joncryl (Figures 7c and 8e), the morphology shows further refinement, with a smoother interface and fewer voids, suggesting that the chain extension reaction has improved interfacial interaction.[50] The more continuous and fibrous morphology seen in the (50/50) blends aligns well with the observed increase in elongation at break.

These enhancements are similar to those reported previously.[33,51] In the current study, tensile strength increases ≈15% and 67% when 1% Joncryl is simultaneously added to the (70/30) PLA/PBAT film and hot-pressed blends, respectively (statistically significant $p < 0.05$ according to ANOVA) (Figure 5d'). This enhancement is ≈38% and ≈65% in (50/50) PLA/PBAT film and hot-pressed blends, respectively (statistically significant $p < 0.05$ according to ANOVA) (Figure 5d). Elongation at break, however, exhibits two different fashions. In film extruded blends, it showed 84% and 22% decrease in (70/30) (Figure 5e') and (50/50) (Figure 5e) series, respectively, upon simultaneously 1 wt.% Joncryl addition. In contrast, in compressed blends, it increased by ≈488% and ≈1000% in (70/30) and (50/50) PLA/PBAT series after 1% of Joncryl, respectively. In comparison, only ≈3% enhancement was observed when 0.75% Joncryl ADR-4370S was simultaneously blended with (70/30) PLA/PBAT blend in the work of Wang et al.[33]

These findings suggest that Joncryl, when introduced under the high-shear and high-orientation conditions of film extrusion, enhances interfacial adhesion and chain interactions but also stiffens the material, limiting chain mobility.

In film-extruded blends, polymer chains are highly oriented due to the shear and elongational forces experienced during processing. This is evident from the SEM images (Figures 7a and 8a). This alignment, particularly in PBAT-rich domains, allows for greater initial extensibility compared to compression-molded samples, where polymer chains remain in a more randomly distributed state. However, Joncryl addition restricts molecular mobility due to chain extension and enhanced PLA-PBAT interactions, reducing elongation at break. It is clearly seen in SEM images how morphology is gradually changed from elongated structures in neat blends into densely populated droplet-like morphologies in Joncryl modified blends (Figures 7b,c and 8b,c). Even though elongation decreases, the pre-existing orientation in film-extruded samples ensures that their extensibility remains higher than that of compression-molded counterparts.

In contrast, compression-molded samples lack significant polymer chain alignment, leading to a lower initial elongation at break. However, with the addition of Joncryl, the improved interfacial adhesion, increased molecular weight, and potential branching mechanisms allow for a greater dissipation of stress during deformation, leading to a progressive increase in elongation at break. This effect is more pronounced in PBAT-rich (50/50) blends, where the inherent ductility of PBAT contributes more significantly to overall strain capacity.

The effect of blend sequence is particularly striking in the tensile strength and elongation at break of the (70/30) PLA/PBAT extruded films results (Figure 5d',e'). The two-step blends, where Joncryl is pre-reacted with either PLA or PBAT before final blending, show the highest tensile strength values, especially in the film-extruded samples. This suggests that pre-modification of one polymer phase facilitates better dispersion of Joncryl, hence more efficient molecular interactions and enhances compatibilization, resulting in a more integrated polymer network. The (PBAT+1J)/PLA blends exhibit the highest tensile strength among all compositions, confirming that sequential compatibilization effectively reduces phase separation and enables better stress transfer across the interface. It is shown that the highest tensile strength (40.82 ± 5.98 MPa) was obtained when 1 wt.% Joncryl was pre-mixed with PBAT in (70/30) (PBAT+1J)/PLA extruded film, compared to its simultaneously blended counterpart, PLA/PBAT/1J, which exhibited values of 35.4 ± 2.52 MPa respectively (Figure 5d'). The elongation at break of this blend (70/30) (PBAT+1J)/PLA film also exhibited a ≈335% increase from its simultaneously blended counterpart (PLA/PBAT/1J) (Figure 5e'). This is while in (70/30) (PLA+1J)/PBAT the increase is ≈491%

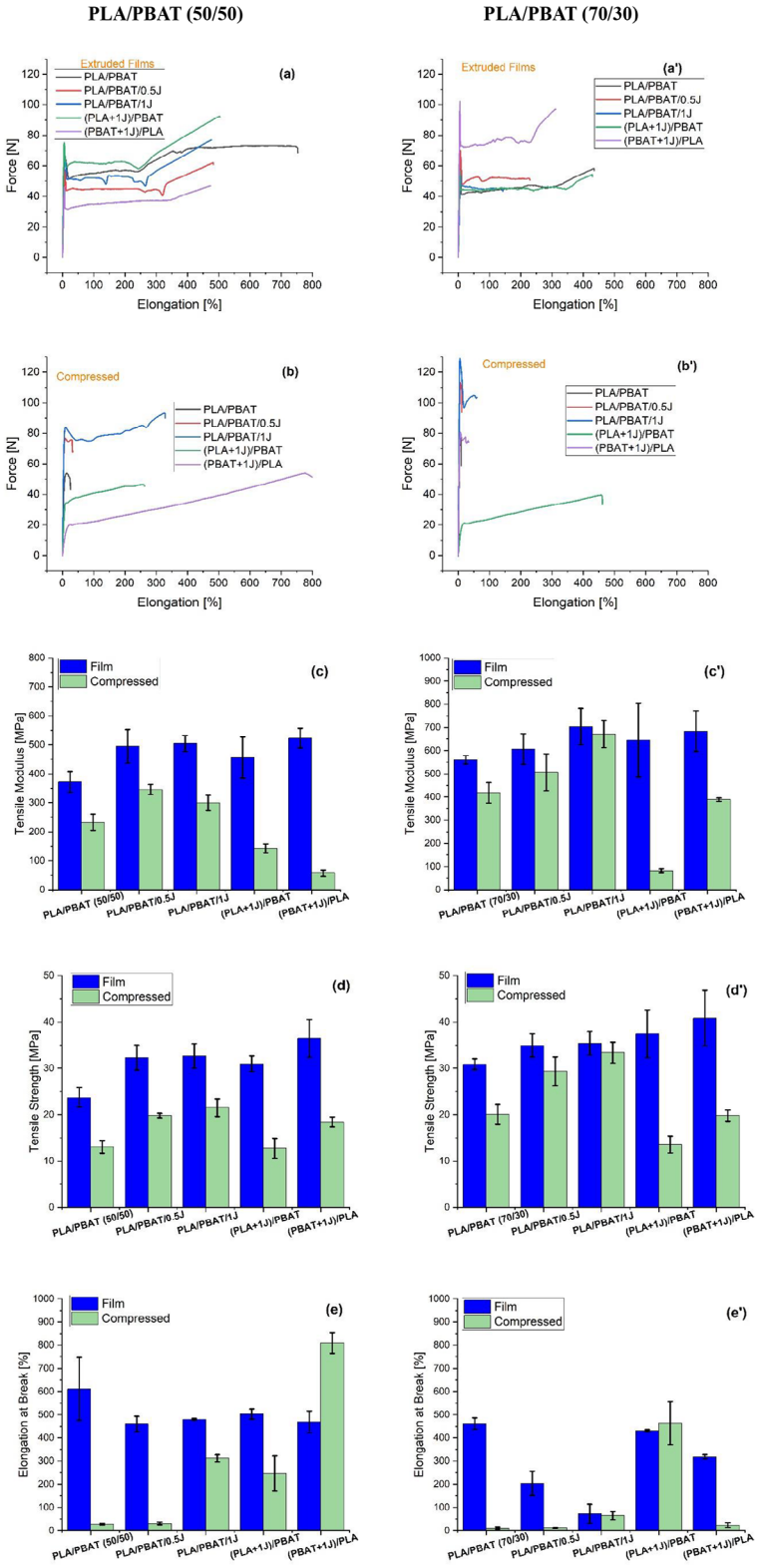

Figure 5. Tensile properties of extruded films and compressed (a–e) (50/50) and (a'–e') (70/30) PLA/PBAT blends incorporated with Joncryl with their sequential blending correspondence.

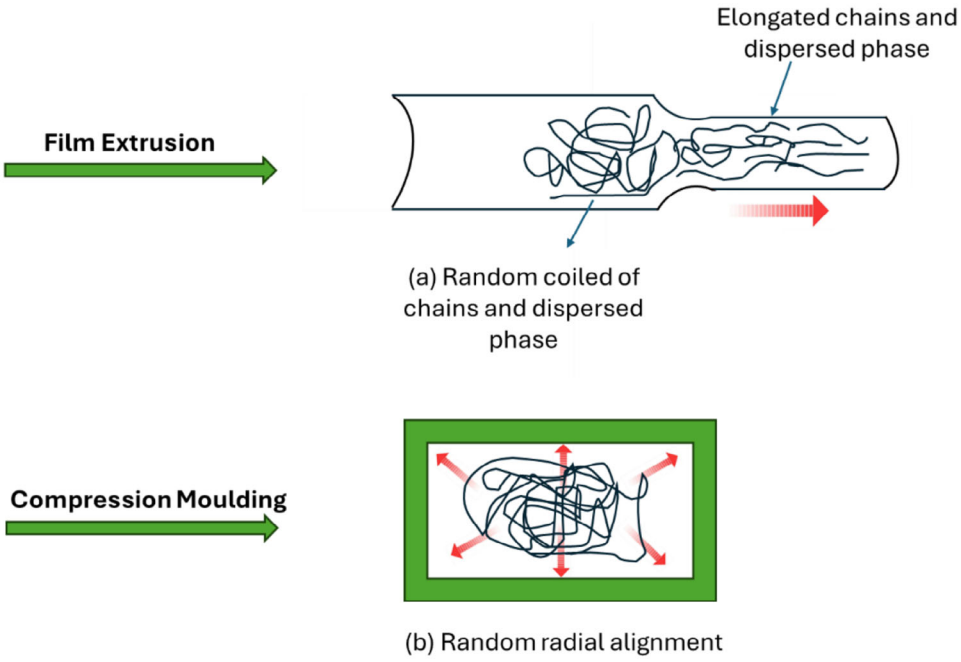

Figure 6. Comparison of polymer alignment during manufacturing via a) film extrusion and b) hot & cold pressing. Red arrows indicate the direction of alignment.

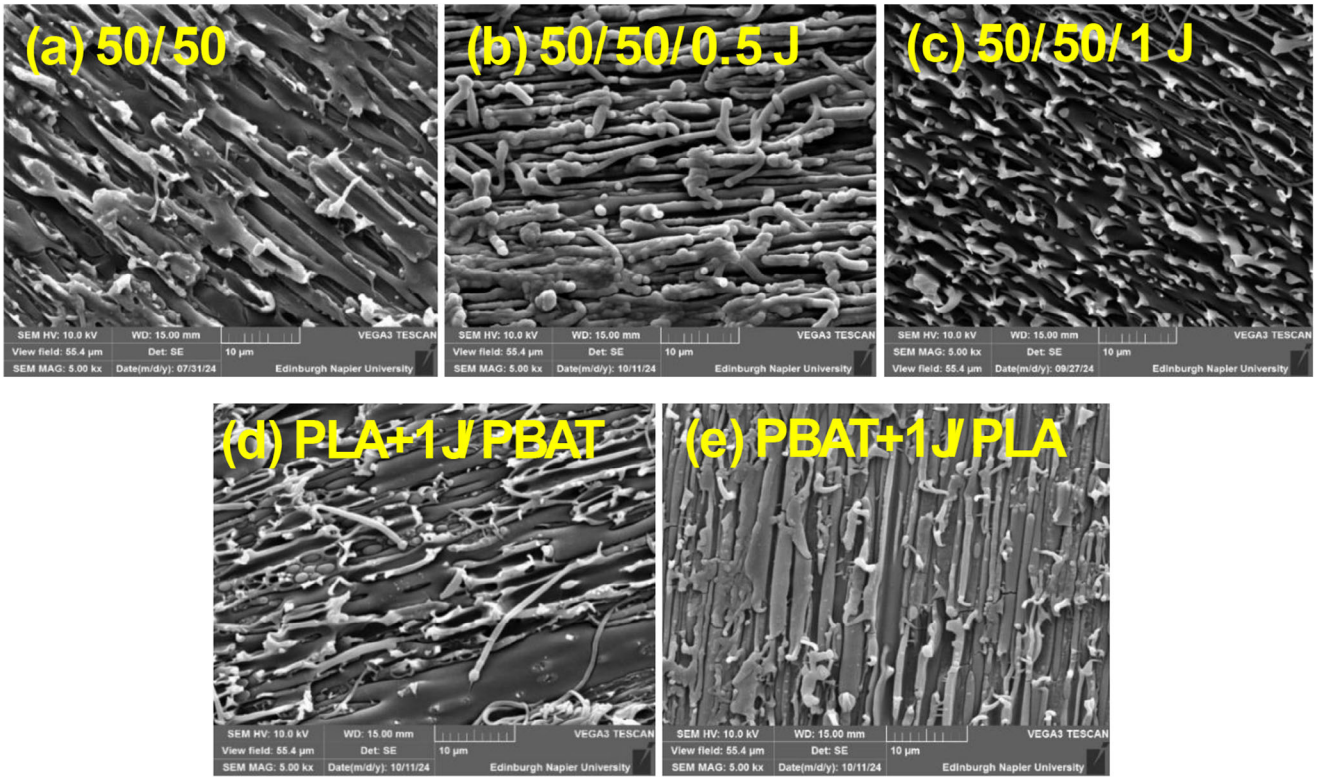

Figure 7. SEM images of the cross-section of cryo-fractured a) (50/50) extruded film simultaneously blended with b) 0.5 wt.% and c) 1 wt. % Joncryl. d,e) representing the sequence blends where Joncryl is pre-blended with either (d) PLA and (e) PBAT. Scale bars are 10 µm in all images.

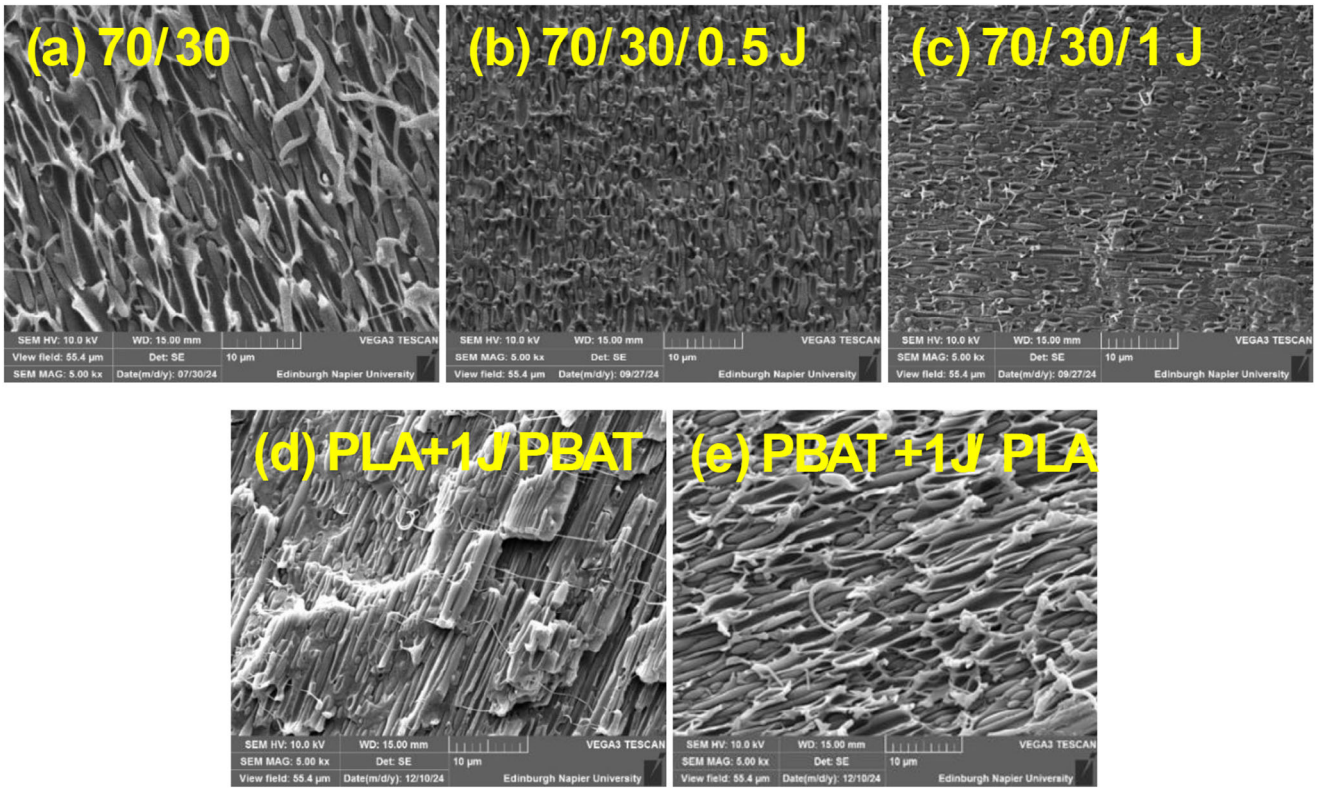

Figure 8. SEM images of the cross-section of cryo-fractured a) (70/30) extruded film simultaneously blended with b) 0.5 wt.% and c) 1 wt. % Joncryl. d,e) representing the sequence blends where Joncryl is pre-blended with either (d) PLA and (e) PBAT. Scale bars are 10 µm in all images.

compared to PLA/PBAT/1J. This is reflected in the SEM images (Figure 8d,e) as well, where the morphology of the blends prepared via sequential addition is drastically changed to highly populated elongated structures without voids. Moreover, it is seen that sequential blending can offer blends with substantially smaller error bars in elongation at breaks when compared to those of simultaneously blended, indicating a more uniform blend can be achieved (Figure 5e'). The elongation results also confirm the strong influence of blend ratio, with (50/50) PLA/PBAT blends consistently exhibiting higher ductility than (70/30) blends, as expected given the inherently flexible nature of PBAT. It is interesting to note that by solely manipulating the processing sequence in the reactive blending of (70/30/1) PLA/PBAT/J film, the elongation at break can reach 431.94 ± 4.56% in (PLA+1% J) PBAT, compared to that of the (50/50) PLA/PBAT blend (611 ± 136%) considering that PBAT content is lower in (70/30). Additionally, the strength is substantially improved, indicating that blends with enhanced properties can be tailored at lower PBAT content when the reactive compatibilizer is introduced in a sequential mode. It is reinforcing the idea that Joncryl's compatibilization effect is more pronounced when it is first reacted with one of the polymer phases.[16,33] The two-step preparation method proved to be significantly more effective than the single-step process for the PLA/PBAT/Joncryl blend, as evidenced by the enhanced mechanical properties achieved. The improved dispersion of Joncryl in the polymer matrix likely promoted stronger interactions between the components, leading to better phase adhesion and, consequently, enhanced mechanical performance. A more detailed comparison between the mechanical performance of (70/30) and (50/50) PLA/PBAT blends is presented in Figure S3 (Supporting Information), where the results are also benchmarked against LDPE films. LDPE was selected as a reference material due to its extensive use in flexible film applications, particularly in packaging, where a balance of strength, flexibility, and processability is required.

The tensile modulus data show that both (70/30) and (50/50) PLA/PBAT blends significantly outperform LDPE, reflecting the inherent stiffness of PLA. Among the blends, the sequentially processed formulations, (PLA+1J)/PBAT and (PBAT+1J)/PLA, exhibit improved strength compared to the conventional PLA/PBAT blend, indicating that controlled compatibilization effectively enhances phase interaction and molecular reinforcement. The tensile strength results demonstrate the advantage of sequentially blended formulations, where (PLA+1J)/PBAT and (PBAT+1J)/PLA (70/30) exhibited ≈173% and ≈198% higher strength than LDPE, respectively, (Figure S3c, Supporting Information) making them excellent candidates for applications where high mechanical integrity is required. A summary of the tensile properties of (70/30) and (50/50) blend series, prepared via film extrusion and compression molding, is provided in Tables S1 and S2 (Supporting Information), respectively.

In contrast, LDPE films maintain higher elongation at break, with values that are ≈56% and 111% higher than (PLA+1J)/PBAT and (PBAT+1J)/PLA (70/30) blends, respectively (Figure S3d, Supporting Information). While this highlights LDPE's superior flexibility, the sequentially blended PLA/PBAT films offer a sig-

nificantly better trade-off between strength and elongation. The ability to achieve a reasonable elongation while simultaneously enhancing tensile strength makes these modified PLA/PBAT blends highly competitive for biodegradable film applications, where mechanical robustness, processability, and environmental sustainability must be balanced.

These results provide a significant breakthrough in understanding the role of processing and blending sequence in tailoring the mechanical properties of PLA/PBAT blends. The film extrusion process clearly outperforms compression molding in producing blends with superior strength and flexibility, highlighting the importance of processing conditions in achieving optimal phase dispersion and interfacial adhesion. More importantly, the sequential (two-step) blending method emerges as a highly effective strategy for maximizing both strength and elongation, offering a refined approach to compatibilization that minimizes phase separation and enhances overall mechanical performance. The PLA+1J/PBAT blend, in particular, demonstrates the most balanced combination of high tensile strength and exceptional elongation, establishing a new standard for reactive compatibilization in biodegradable polymer systems. These findings have profound implications for the development of PLA/PBAT blends for flexible film applications, where achieving a balance between strength and ductility is critical for functionality and durability.

Building on the insights gained from the film-extruded blends, the next focus will be on the mechanical performance and morphological characteristics of injection-molded (70/30) PLA/PBAT blends modified with 0.5 and 1 wt.% Joncryl. The decision to emphasize this composition, rather than the (50/50) blends, stems from the goal of achieving the most efficient compatibilization while maintaining a lower PBAT content to balance mechanical strength and flexibility. However, rather than revisiting the PLA+J/PBAT formulation, which previously showed the most striking results in terms of both strength and elongation, the focus shifts toward (PBAT+J)/PLA for this stage of the study. This shift is driven by both practical and industrial considerations, ensuring that the proposed formulation aligns with large-scale processing constraints.

One critical factor influencing this decision is the thermal stability of PLA, which is more prone to degradation under multiple processing steps compared to PBAT. In a two-step blending approach, where one component is pre-mixed with Joncryl before final blending, pre-dispersing PBAT with Joncryl before mixing it with PLA offers a significant advantage by mitigating PLA's degradation risk during the second processing step. This strategy not only preserves the structural integrity of PLA but also provides a more industrially relevant approach where polymer degradation must be minimized in repeated processing cycles. Additionally, FTIR results from earlier sections suggested that Joncryl exhibits a higher reactivity toward PLA than PBAT, indicating that a progressive reaction mechanism could be exploited in this blend sequence.

The tensile results and SEM analysis of PLA/PBAT blends with Joncryl reveal significant improvements in mechanical performance and blend morphology, particularly with the two-step blending process. While the modulus and strength of the blends remain unchanged (**Figure** 9b,d), the stress at break and elongation at break show remarkable enhancements of 71% and 75%, respectively (Figure 9c,e) compared to the simultaneously blended PLA/PBAT/0.5J. The addition of Joncryl improves the stress at break, with the two-step method showing the most significant increase due to the enhanced compatibilization and interfacial interaction between PLA and PBAT. This improvement can be attributed to the pre-dispersion of Joncryl with PBAT, which ensures a more cohesive structure and better stress distribution. The elongation at break is significantly enhanced across all Joncryl-modified blends, with the two-step method demonstrating exceptional ductility and strain hardening behavior. This strain hardening indicates that the material exhibits increasing resistance to deformation under tensile loading, reflecting improved energy dissipation and toughness.[16] A summary of the tensile properties of the (70/30) blend series, prepared via injection molding, is presented in Table S3 (Supporting Information).

The superior mechanical properties observed in the two-step blend are strongly supported by SEM analysis conducted after sample rupture under both tensile and impact loads (**Figure 10**). The SEM image shows a uniform and cohesive morphology, with no evidence of large voids or phase separation (Figure 10d'), indicating excellent dispersion and interaction between the PLA and PBAT phases. The morphology of the impact fractured surfaces exhibits a gradual transition from a nodular to a fibrillar form, as observed in the simultaneous and two-step blends. In the simultaneous blend, the fracture surfaces are more nodular, which is indicative of a more brittle failure. However, in the two-step blends, the fracture morphology shifts toward a fibrillar structure, suggesting increased ductility. The presence of elongated fibrils in the fracture surface is characteristic of a material undergoing plastic deformation before failure, highlighting the improved energy absorption and the flexible nature of the sample. This change in morphology is a clear indication of enhanced toughness due to the improved interfacial adhesion and blend compatibility. A similar trend of morphology change from droplet to fibrillar form has been observed and confirmed in other studies.[33,39,46]

3.3. Thermal Properties

The DSC results reveal important insights into how the addition of Joncryl and different blending sequences influence the crystallization and melting behavior of (70/30) and (50/50) PLA/PBAT extruded blends as well as (70/30) injection molded blends (**Figures 11** and **12**). The heating and cooling scans provide a detailed understanding of how compatibilization affects the molecular arrangement, phase interactions, and thermal transitions in these biodegradable polymer systems. The glass transition temperature (T_g) of PLA remains largely unchanged across all samples, suggesting that the presence of Joncryl does not significantly influence the segmental mobility of the polymer chains at this temperature range. **Tables 3** and **4** show the thermal properties of (70/30) and (50/50) PLA/PBAT extruded films, respectively. while **Table 5** shows the thermal properties of the (70/30) injection molded blends.

The cooling scans provide further confirmation of the impact of Joncryl and the blending sequence on the crystallization behavior. The T_c shifts to lower values upon Joncryl addition, suggest-

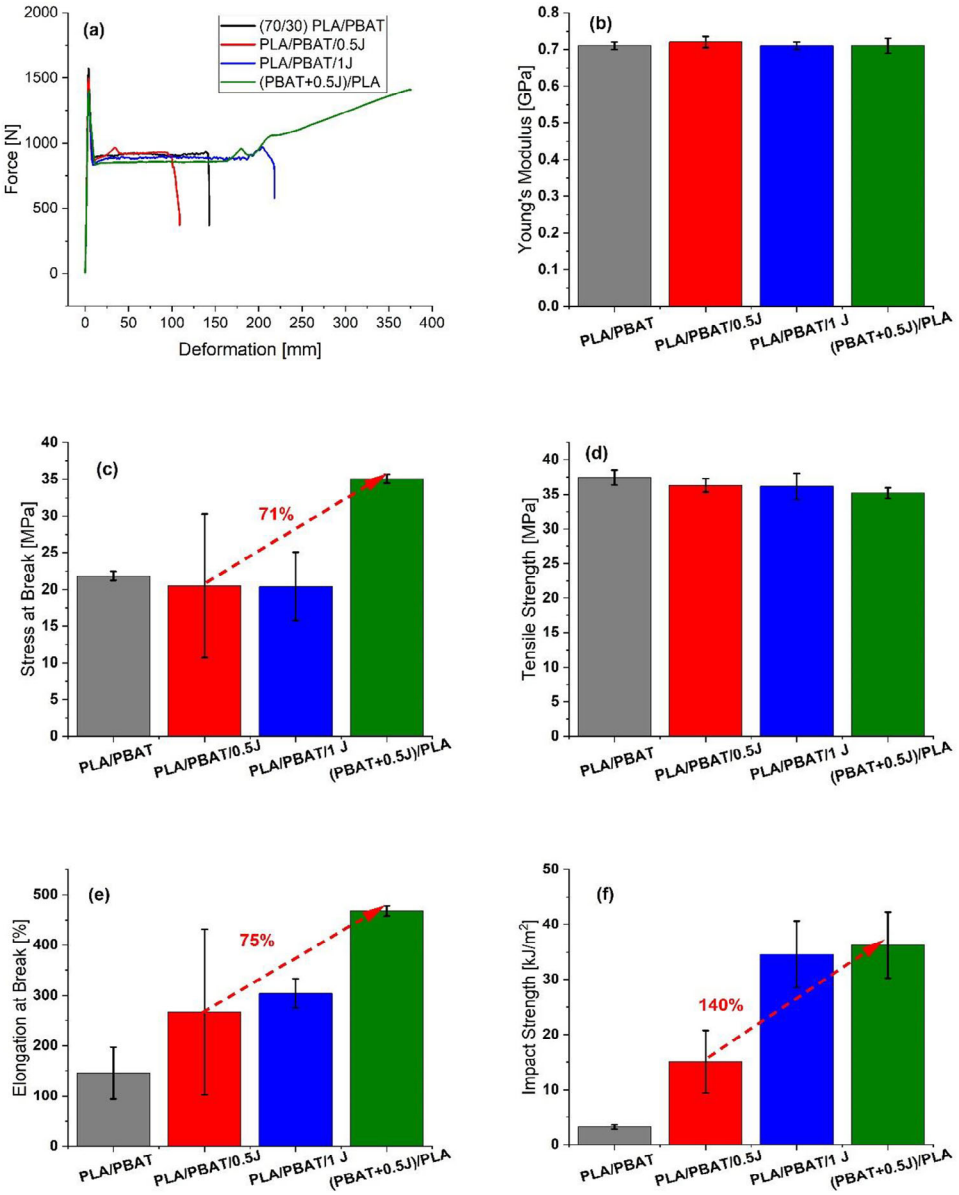

Figure 9. a) tensile curves, b) tensile modulus, c) stress at break, d) tensile strength, e) elongation at breaks, and f) impact strength of injection molded (70/30) PLA/PBAT blends.

ing that the compatibilization process delays the onset of crystallization, making it less efficient. Similar observations were reported, where the addition of chain extenders lowered the T_c of such blends, suggesting that crystallization became more difficult due to the higher molecular weight of the blends with chain extenders.[52,53] This shift to lower crystallization temperatures is even more pronounced in the two-step blending sequences, reinforcing the idea that modifying the polymer chains before final blending creates a more hindered crystallization process. In the (50/50) PLA/PBAT series, the neat blend exhibits a T_c of 82.05 °C, while in (PLA+J)/PBAT, T_c decreases to 71.50 °C, and in (PBAT+J)/PLA, Tc shifts to 73.56 °C. This downward shift confirms that Joncryl disrupts the crystallization process by modifying the polymer structure, increasing molecular weight, and reducing the ability of PLA chains to reorganize into crystalline domains.[12,53] This aligns well with our previous study, where the T_c of PBAT and PBAT/J shifted to higher temperatures, by more than 10 degrees, after six injection cycles, indicating that degradation and reduced molecular weight were responsible for these shifts.[54] In contrast, the current work shows hindered crystallization.

A similar trend is observed in the (70/30) PLA/PBAT series, where the crystallization temperature also decreases upon Joncryl addition. The degree of T_c suppression is greater in (PBAT+J)/PLA compared to (PLA+J)/PBAT, further indicating that the sequence of compatibilization plays a role in how the molecular structure evolves. These results confirm that pre-dispersing Joncryl with PBAT introduces a greater level of structural hindrance than pre-reacting it with PLA, leading to a more pronounced suppression of crystallization.

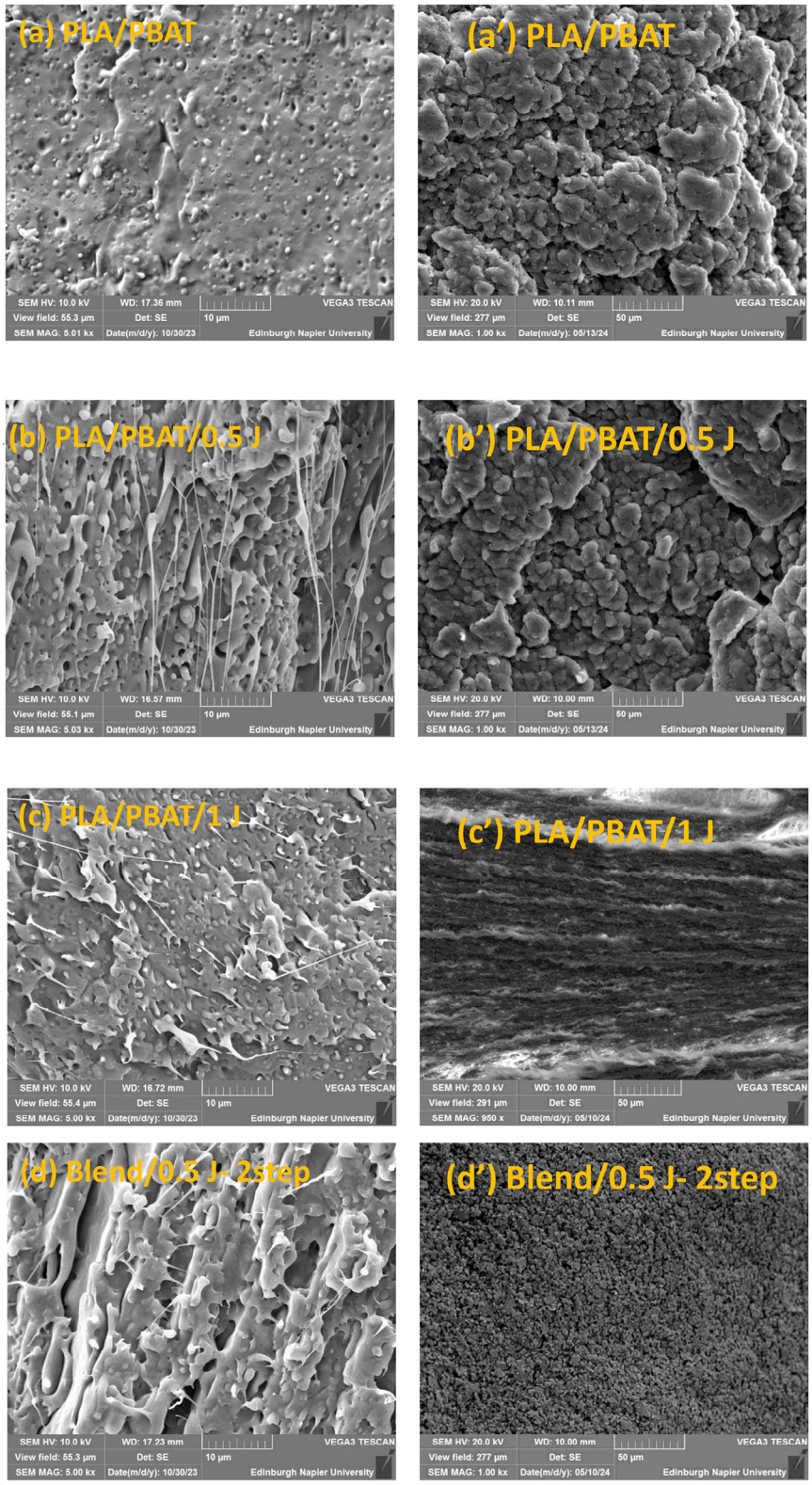

Figure 10. SEM images of the cross-section of impact fractured (a–d) and tensile fractured (a'–d') injection molded blends. The scale bars represent 10 µm in Figure (a–d) and 50 µm in Figure (a'–d').

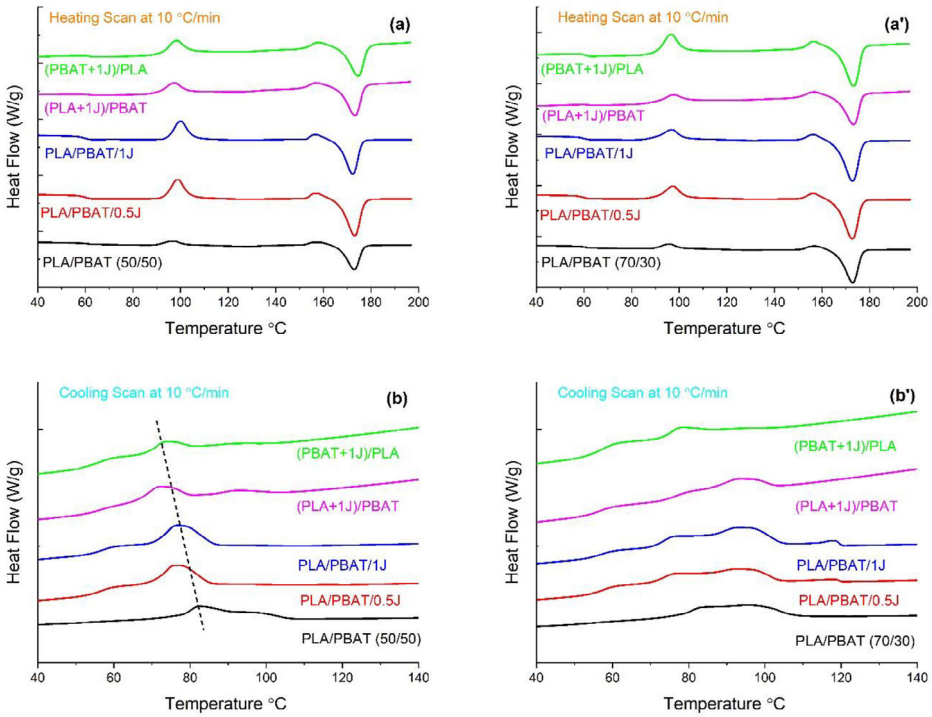

Figure 11. DSC thermograms of extruded films (a,b) (50/50) and (a',b') (70/30). (a,a') are showing the heating and (b, b') the cooling scans at a rate of 10 °C min^{-1}.

The DSC results, when considered alongside FTIR, mechanical, and SEM data, reveal a more comprehensive understanding of how sequential blending impacts the crystallization behavior of PLA/PBAT/Joncryl blends. While the (70/30) sequential blends, particularly (PLA+1J)/PBAT film and (PBAT+0.5 J)/PLA injection molded blend, show a decrease in PLA crystallinity, this does not contradict the findings that these blends exhibit better phase interaction, improved elongation at break, while maintaining the tensile strength. Instead, it reinforces the idea that effective compatibilization alters the molecular architecture in a way that enhances mechanical properties while suppressing crystallinity.

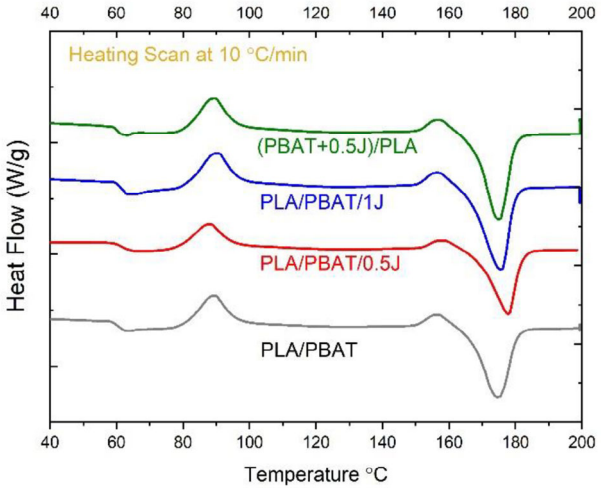

Figure 12. DSC thermograms of the injection molded (70/30) PLA/PBAT blends.

Despite the decrease in crystallinity in sequentially blended (70/30) formulations, their mechanical properties, particularly strength, improved in the extruded films. This phenomenon can be explained by the role of crystallinity in mechanical behavior. High crystallinity in PLA often correlates with higher stiffness but increased brittleness, whereas a reduction in crystallinity typically leads to increased chain mobility, better energy dissipation, and enhanced elongation at break. Therefore, while PLA crystallization is somewhat restricted in the (PLA+1J)/PBAT film and (PBAT+0.5 J)/PLA injection molded, this does not negatively impact its performance but rather facilitates a more ductile, tougher material with improved mechanical properties.

This stands in contrast to the (50/50) PLA/PBAT blends, where crystallinity gradually increased in sequential blending. In these blends, the presence of a higher PBAT fraction provides more molecular flexibility, allowing PLA chains to still crystallize effectively despite compatibilization. The sequential process in the (50/50) blends enables PLA to retain better crystallization ability, which is reflected in the increase in the degree of crystallinity (χ%) in (PBAT+1J)/PLA. The shift in T_c to lower values in sequentially blended (70/30) formulations also aligns with these observations. The fact that sequentially blended (70/30) samples perform better mechanically despite reduced crystallinity confirms that the key factor driving performance is improved interfacial adhesion and phase integration rather than crystallization itself.

Taken together, the findings illustrate that effective compatibilization, as evidenced by FTIR peak shifts, improved mechanical performance, and refined SEM morphologies, is not nec-

Table 3. Thermal properties of (70/30) PLA/PBAT blends.

Blend	T_g [°C]	T_{cc} [°C]	Δ_{Hcc} J/g	Δ_{Hm} J/g	T_{c1} [°C]	T_m [°C]	χ%
PLA/PBAT (70/30)	60.66	96.22	4.15	31.07	95.64	172.76	41.35
PLA/PBAT/0.5 J	60.60	97.19	11.43	40.98	96.30	172.68	45.39
PLA/PBAT/1J	59.57	96.72	9.27	40.28	96.16	172.71	47.63
(PLA+1J))/PBAT	62.22	97.06	7.55	30.46	92.93	173.10	35.19
(PBAT+1J))/PLA	61.03	96.30	16.16	41.44	77.20	173.11	38.83

Table 4. Thermal properties of (50/50) PLA/PBAT blends.

Blend	T_g [°C]	T_{cc} [°C]	Δ_{Hcc} J/g	Δ_{Hm} J/g	T_{c1} [°C]	T_m [°C]	χ%
PLA/PBAT (50/50)	61.01	97.26	3.63	20.28	82.05	172.77	35.81
PLA/PBAT/0.5 J	60.49	98.76	14.90	23.23	76.10	173.10	17.91
PLA/PBAT/1J	59.17	99.87	14.40	30.73	76.65	172.23	35.12
(PLA+1J))/PBAT	61.33	97.00	8.60	27.03	71.50	173.22	39.63
(PBAT+1J))/PLA	61.80	97.94	11.34	28.97	73.56	174.50	37.91

essarily correlated with increased crystallinity. In fact, in PLA-rich blends like (70/30), excessive crystallinity can lead to embrittlement, while controlled reduction in crystallinity due to compatibilization results in superior ductility and toughness. This provides a major breakthrough in understanding the balance between crystallization, compatibilization, and mechanical properties, particularly in biodegradable polymer blends where processing conditions significantly influence final material behavior. Ultimately, the results demonstrate that effective compatibilization via sequential blending can override the negative effects of reduced crystallinity by enhancing phase adhesion, stress distribution, and overall toughness. Meanwhile, in (50/50) blends, where PLA crystallization is less restricted, sequential blending enhances crystallinity, further supporting that the impact of compatibilization is composition dependent. These results highlight the need for tailored compatibilization strategies based on blend composition, ensuring that both structural and mechanical properties are optimized for specific applications.

It is worth mentioning that the decrease in crystallinity not only enhances elongation and toughness but also improves environmental performance. In biodegradable polymers, lower crystallinity facilitates enzymatic attack and microbial degradation, as amorphous regions are more accessible. It is well established that amorphous regions degrade more readily than crystalline domains due to their higher susceptibility to enzymatic attack and hydrolytic degradation, making this formulation particularly promising for biodegradable packaging and sustainable polymer applications.[55] The restricted crystallization observed in this blend suggests a higher proportion of amorphous regions, which could facilitate faster water diffusion and enzymatic penetration, thereby enhancing the overall biodegradation rate. This can be the scope of a future study to correlate the blending strategies with biodegradability.

The findings from injection molding elucidate the structural advantages of sequence-controlled compatibilization in thicker parts, where orientation effects influence performance, while highlighting why hot-pressed blends may not achieve optimal results due to their lack of shear-induced alignment (e.g., trays, lids, or containers). This holistic approach provides valuable insights into how PLA/PBAT blends can be engineered for both flexible film applications and rigid components, ensuring that the material remains viable across a range of industrial and commercial uses.

4. Conclusion

This study systematically investigated the impact of processing sequence and manufacturing methods on the mechanical, morphological, and thermal properties of PLA/PBAT blends modified with Joncryl. Various processing techniques, including film extrusion, compression molding, and injection molding, were employed to evaluate the compatibilization efficiency of Joncryl under different conditions. The two-step blending approach, in which Joncryl was pre-reacted with either PLA or PBAT before final blending, demonstrated superior dispersion and interfacial adhesion compared to the single-step method. These results highlight the critical role of the processing approach in tailoring the properties of biodegradable polymer blends for high-performance applications.

Table 5. Thermal properties of the injection molded (70/30) PLA/PBAT bends.

Blend	T_{cc} [°C]	Δ_{Hcc} J/g	Δ_{Hm} J/g	T_m [°C]	χ%
PLA	89.22	26.99	56.58	174.50	31.78
PLA/PBAT (70/30)	95.91	18.38	43.34	175.16	38.30
PLA/PBAT/0.5 J	97.94	23.72	49.31	177.14	39.27
PLA/PBAT/1 J	89.95	21.64	47.46	175.40	39.63
(PBAT+0.5J))/PLA	89.00	15.37	30.23	175.03	22.81

Table 6. Summary of mechanical properties and packaging recommendations for PLA/PBAT-based blends processed via film extrusion and injection molding at a 70/30 blend ratio.

Blend	Manufacturing method	Property summary	Recommendation for use in packaging
PLA/PBAT/1J (70/30)	Film Extrusion	High modulus and strength, low elongation	Suitable for semi-rigid packaging (trays, lids).
(PLA+1J)/PBAT (70/30)	Film Extrusion	Good balance of stiffness, strength, and flexibility	Best for flexible food packaging applications.
(PBAT+1J)/PLA (70/30)	Film Extrusion	Balanced properties, very strong & moderate elongation	Suitable for semi-rigid packaging requiring durability.
(PBAT+0.5J)/PLA (70/30)	Injection molding	Strong, very tough, and high elongation	Best for rigid packaging applications (e.g., cutlery, containers).

The two-step blending method significantly improved interfacial adhesion and mechanical performance, particularly in (PLA+1J)/PBAT and (PBAT+1J)/PLA blends. Tensile strength of (70/30) blends increased by ≈15% and 67% in extruded films and hot-pressed blends, respectively, upon simultaneous blending with 1 wt.% Joncryl.

The film-extruded samples exhibited superior mechanical properties due to shear-induced molecular orientation and improved phase dispersion. In contrast, compression-molded blends showed lower tensile strength, modulus, and elongation at break than the extruded films.

The tensile strength results demonstrate the advantage of sequentially blended formulations, where (PLA+1J)/PBAT and (PBAT+1J)/PLA (70/30) exhibited ≈173% and ≈198% higher strength than LDPE, respectively.

Injection-molded samples demonstrated enhanced impact resistance and elongation at break. The (PBAT+J)/PLA blend showed a 75% and 140% increase in elongation at break and impact strength compared to simultaneously blended counterparts.

SEM analysis demonstrated that two-step blended samples had refined phase morphology with fewer voids, contributing to improved stress distribution and mechanical integrity.

DSC analysis revealed that sequential blending led to a decrease in PLA crystallinity, resulting in enhanced flexibility. The T_c decreased more significantly in (PBAT+J)/PLA blends, confirming a greater level of structural hindrance due to effective compatibilization.

The findings of this study provide a strong foundation for the development of advanced biodegradable polymer blends with optimized mechanical and thermal properties. The improved phase dispersion and interfacial adhesion achieved through sequential blending can be further explored in large-scale applications such as flexible packaging and agricultural films. **Table 6** shows an overview of mechanical properties and packaging recommendations for PLA/PBAT blends (70/30 ratio) processed through film extrusion and injection molding. Additionally, the impact of processing history on long-term biodegradability and recyclability warrants further investigation. Future research could focus on extending these compatibilization strategies to other biopolymer systems and exploring the potential of sustainable additives to further enhance performance and environmental impact.

Supporting Information

Supporting Information is available from the Wiley Online Library or from the author.

Conflict of Interest

The authors declare no conflict of interest.

Data Availability Statement

The data that support the findings of this study are available in the supplementary material of this article.

Keywords

blending sequence, compatibilization, compression molding, film extrusion, injection molding, Joncryl ADR 4468, PLA/PBAT

Received: March 9, 2025
Revised: April 20, 2025
Published online:

[1] D. K. Schneiderman, M. A. Hillmyer, *Macromolecules* **2017**, *50*, 3733.
[2] G. Kale, T. Kijchavengkul, R. Auras, M. Rubino, S. E. Selke, S. P. Singh, *Macromol. Biosci.* **2007**, *7*, 255.
[3] W. Chen, C. Qi, Y. Li, H. Tao, *Radiat. Phys. Chem.* **2021**, *180*, 109239.
[4] S. J. Barnes, *Environ. Pollution* **2019**, *249*, 812.
[5] W. Wang, J. Ge, X. Yu, H. Li, *Sci. Total Environ.* **2020**, *708*, 134841.
[6] Y. Zhou,G. He, X. Jiang, L. Yao, L. Ouyang, X. Liu, W. Liu, Y. Liu, *J. Hazard. Mater.* **2021**, *411*, 125178.
[7] P. Li, X. Wang, M. Su, X. Zou, L. Duan, H. Zhang, *Bull. Environ. Contam. Toxicol.* **2021**, *107*, 577.
[8] V. T. Weligama Thuppahige, M. A. Karim, *Comprehensive Revi. Food Sci. Food Safety* **2022**, *21*, 689.
[9] K. Cai, X. Liu, X. Ma, J. Zhang, S. Tu, J. Feng, *Polymer* **2024**, *291*, 126587.
[10] V. Siracusa, P. Rocculi, S. Romani, M. Dalla Rosa, *Trends Food Sci. Technol.* **2008**, *19*, 634.
[11] S. Mangaraj, A. Yadav, L. M. Bal, S. K. Dash, N. K. Mahanti, *J. Packag. Technol. Res.* **2019**, *3*, 77.
[12] M. Kumar, S. Mohanty, S. K. Nayak, M. R. Parvaiz, *Bioresour. Technol.* **2010**, *101*, 8406.
[13] M. Nofar, M. C. Heuzey, P. J. Carreau, M. R. Kamal, J. Randall, *J. Rheol.* **2016**, *60*, 637.
[14] R. Al-Itry, K. Lamnawar, A. Maazouz, N. Billon, C. Combeaud, *Eur. Polym. J.* **2015**, *68*, 288.
[15] Y. Ding, B. Lu, P. Wang, G. Wang, J. Ji, *Polym. Degrad. Stab.* **2018**, *147*, 41.
[16] L. C. Arruda, M. Magaton, R. E. Bretas, M. M. Ueki, *Polym. Test.* **2015**, *43*, 27.
[17] N. Zhang, Q. Wang, J. Ren, L. Wang, *J. Mater. Sci.* **2009**, *44*, 250.
[18] S. Y. Gu, K. Zhang , J. Ren, H. Zhan, *Carbohydr. Polym.* **2008**, *74*, 79.

[19] H. T. Chiu, S. Y. Huang, Y. F. Chen, M. T. Kuo, T. Y. Chiang, C. Y. Chang, Y. H. Wang, *Int. J. Polym. Sci.* **2013**, *2013*, 951696.
[20] H. R. Yang, G. Jia, H. Wu, C. Ye, K. Yuan, S. Liu, L. Zhou, H. Xu, L. Gao, J. Cui, S. Fang, *Mater. Lett.* **2022**, *329*, 133067.
[21] S. Su, *Polymers* **2021**, *13*, 2339.
[22] S. Su, M. Duhme, R. Kopitzky, *Materials* **2020**, *13*, 4897.
[23] C. Aversa, M. Barletta, G. Cappiello, A. Gisario, *Eur. Polym. J.* **2022**, *173*, 111304.
[24] S. Sinha Ray, M. Bousmina, *Macromol. Rapid Commun.* **2005**, *26*, 450.
[25] F. Tao, D. Auhl, A. C. Baudouin, F. J. Stadler, C. Bailly, *Macromol. Chem. Phys.* **2013**, *214*, 350.
[26] S. Aparna, D. Purnima, R. B. Adusumalli, *Polym.-Plast. Technol. Eng.* **2017**, *56*, 617.
[27] G. Fredi, A. Dorigato, *Adv. Ind. Eng. Polym. Res.* **2024**, *7*, 373.
[28] M. M. Coleman, P. C. Painter, J. F. Graf, *Specific Interactions and the Miscibility of Polymer Blends*, Technomic Publishing Co., Lancaster, Pennsylvania **2017**.
[29] R. Al-Itry, K. Lamnawar, A. Maazouz, *Polym. Degrad. Stab.* **2012**, *97*, 1898.
[30] F. ALPdL, L. R. Tonini Filho, P. S. Calvao, A. M. de Souza, *Polym. Test.* **2017**, *62*, 189.
[31] S. Soleymani Eil Bakhtiari, I. Shyha, D. Sun, M. Nofar, R. Salehiyan, *Adv. Ind. Eng. Polym. Res.* **2025**. https://doi.org/10.1016/j.aiepr.2025.03.001
[32] H. Li, M. A. Huneault, *J. Appl. Polym. Sci.* **2011**, *122*, 134.
[33] X. Wang, S. Peng, H. Chen, X. Yu, X. Zhao, *Composites, Part B* **2019**, *173*, 107028.
[34] R. Al-Itry, K. Lamnawar, A. Maazouz, *Rheol. Acta* **2014**, *53*, 501.
[35] C. Total, Product Data Sheet, Luminy(R)L130, www.total-corbion.com pla@total-corbion.com.
[36] Global Marketing Biopolymers, www.ecoflex.basf.com.
[37] S. Körber, K. Moser, J. Diemert, *Polymers* **2022**, *14*, 384.
[38] J. M. Raquez, Y. Habibi, M. Murariu, P. Dubois, *Prog. Polym. Sci.* **2013**, *38*, 1504.
[39] D. Jubinville, M. Awad, H. S. Lee, T. H. Mekonnen, *J. Polym. Environ.* **2024**, *32*, 5857.
[40] S. Chopra, K. Pande, P. Puranam, A. D. Deshmukh, A. Bhone, R. Kale, A. Galande, B. Mehtre, J. Tagad, S. Tidake, *RSC Adv.* **2023**, *13*, 7135.
[41] A. L. P. d. L. Freitas, L. R. Tonini Filho, P. S. Calvao, A. M. de Souza, *Polym. Test.* **2017**, *62*, 189.
[42] J. M. Wang, H. Wang, E. C. Chen, Y. J. Chen, T. M. Wu, *Polymers* **2020**, *12*, 1968.
[43] J. W. Robinson, E. M. Frame, G. M. Frame, M. Eileen, F. Skelly, *Undergraduate Instrumental Analysis*, CRC Press, Boca Raton, NY, USA **2005**
[44] T. Kijchavengkul, R. Auras, M. Rubino, *Polym. Test.* **2008**, *27*, 55.
[45] M. E. Grigora, Z. Terzopoulou, K. Tsongas, P. Klonos, N. Kalafatakis, D. N. Bikiaris, A. Kyritsis, D. Tzetzis, *Polymers* **2021**, *13*, 1381.
[46] Y. Han, J. Shi, L. Mao, Z. Wang, L. Zhang, *Ind. Eng. Chem. Res.* **2020**, *59*, 21779.
[47] J. E. Choo, T. H. Park, S. M. Jeon, S. W. Hwang, *J. Polym. Environ.* **2023**, *31*, 4007.
[48] X. Li, X. Ai, H. Pan, J. Yang, G. Gao, H. Zhang, H. Yang, L. Dong, *Polym. Adv. Technol.* **2018**, *29*, 1706.
[49] W. Liu, Y. Wang, S. Xiang, H. Liu, *Polymer* **2024**, *296*, 126815.
[50] X. Chen, Z. Zeng, Y. Ju, M. Zhou, H. Bai, Q. Fu, *Polymer* **2023**, *266*, 125620.
[51] A. Altınbay, C. Ozsaltik, D. Jahani, M. Nofar, *Int. J. Biol. Macromol.* **2025**, *303*, 140703.
[52] B. Nekhamanurak, *Mater. Res. Express* **2022**, *9*, 064002.
[53] J. M. F. da Silva, B. G. Soares, *Polym. Test.* **2021**, *93*, 106889.
[54] R. Salehiyan, M. C. Kim, T. Xia, S. Jin, M. Nofar, L. Chalmers, K. Hyun, *Polym. Eng. Sci.* **2025**, *65*, 1187.
[55] D. Sun, T. Henthorn, C. M. Popescu, R. Salehiyan, *Appl. Sci.* **2025**, *15*, 2951.

